Relationships Between Constitutive Equations of the Microcracked Process Zone and the Toughness of Ceramics and Concrete

F.E. Buresch

Kernforschungsanlage Jülich GmbH, Institut für Reaktorwerkstoffe, Postfach 1913, D-5170 Jülich, Germany

Abstract

It is proposed that the crack resistance of ceramics and cementitious materials is governed by local parameters of microcrack configurations inside the process zone ahead of a growing macrocrack. Spontaneous and stress-induced microcracks develop from microcrack nuclei at critical levels of the residual strain-induced energy release rate. Microcrack nuclei are residual stress-induced stress concentrations on microstructural inhomogeneities. The metastable pinned microcracks form into a microcrack system inside the frontal process zone. The local parameters of this microcrack system such as the density length and elastic interaction of the microcracks determine the constitutive equations of the microcrack system and the crack resistance of the material.

1. Introduction

Polycrystal one or multiphase ceramics fatigue under static or cyclic loading well below the fracture load. This is a consequence of growing natural or spontaneous cracks but mainly of stress-induced cracks /1/. Phenomenologically the same features are observed in cementitious materials such as mortar and concrete /2, 3/. Stress-induced microcracks develop from microcrack nuclei. These are residual strain induced stress concentrations on microstructural inhomogeneities such as triple points of grain boundaries or pores. Residual strains ε are a consequence of the thermomechanical incompatability of adjacent grains or phases in facets due to volume shrinkage typical of this class of materials during fabrication such as sintering or hydration /2-4/.

Spontaneous and/or stress-induced microcracking develops from microcrack nuclei at discrete values of the residual strain-induced energy release G_{Ir}. The density of these metastable pinned microcracks is extremely high in the highly stressed region of the frontal process zone /2, 5, 6/. Thus a microcrack system develops in this zone. The local parameters of these crack systems, such as the length and density of the cracks, as well as the integral parameters of the crack system, such as the stress intensity factor, determine the crack resistance of these classes of materials /6/. This will be exemplified in the following thereby relating microstructural, microcrack field and crack resistance parameters to each other.

2. Relations between microstructural features and microcrack parameters of the frontal process zone

Following the range of residual strain-induced energy release rates a critical grain size d_c is characteristic of spontaneous microcracking. This is expressed by the equation

$$G_{Irc} = \frac{E\,\varepsilon^2 A^2 d_c}{24\,(1-v^2)} \geq 2\,\gamma_s \qquad \text{eq. (1)}$$

where E, v are elastic parameters, γ_s is the specific surface energy, and ε is the residual strain as mentioned above and A is the anisotropy factor introduced by Davidge et al /7/. $A \leq 1$ is a measure of the statistical orientation of adjacent grains in facets due to orientation differences in a nearly isotropic microstructure. G_{Ir} as a function of measured grain size distributions is shown in Fig. 1 for zirconia-toughened alumina, pure alumina and concrete with values for the parameters of eq. (2) from the literature as shown in Tab. 1. Thus the critical grain size d_c for spontaneous microcracking of the above mentioned materials is in the range of 0.5 to 1 µm, 80 to 100 µm and about 25 mm respectively /4, 6/.

Generally the residual strain-induced tension and compression stresses are in equilibrium in each facet after fabrication. However, this equilibrium is disturbed under the action of the main principal tension stress of an external load also causing microcracking of facets which are adjacent to grains of sizes $d < d_c$, that means values of $G_{Ir} < G_{Irc}$. Thus the crack resistance of this class of materials is, with increasing external stress intensity, a function of the grain facet size given as

$$J_R = \frac{K_I^2\,(1-v^2)}{E} + \frac{E\,\varepsilon^2 A^2 d}{24\,(1-v^2)} \geq 2\,\gamma_s \qquad \text{eq. (2)}$$

The evaluation of a stress-induced microcrack field measured with acoustic emission analyses during loading of a specimen is well-known from data in the literature /1, 2/. From this it was recognized that microcracking often commences at stress levels well below 50 % of the strength of these materials /3/. However, with increasing K_I unbroken facets may always exist adjacent to small grains of a microstructure. These facets are given by the equation

$$A^2 d_n \leq \frac{1}{G_{Ir\,max}} \left(\frac{K_I^2 (1-v^2)}{E} - J_R \right) \qquad \text{eq. (3)}$$

Here in the terms

$$d_n^+ = \frac{d_n}{d_{max}} \quad \text{and} \quad G_{Ir\,max} = \frac{E\,\varepsilon^2\,d_{max}}{24\,(1-v^2)} \qquad \text{eq. (4)}$$

are d_{max} the maximum grain of the respective grain size distribution and A = 1. d_n is the lower bound of the n^{th} grain size class of the grain size distribution of the microstructure. Thus the n class of grain size of a grain size distribution characterizes n fictitious levels of residual energy release rates G_{Irn}, which are defined by the normalized parameter $A^2 d_n^+$. Only the external stress-induced discrete levels of residual energy rates which are greater than a specific value of $A^2 d_n^+$ activate microcracking which contributes to the crack resistance of the material. Fig. 2 shows as an example the microcrack density of a duplex microstructure as a function of the grain size distribution if an increasing number of grain size class (n = 4 ... 8) contributes to microcracking.

3. The influence of microcrack field parameters of the process zone on the crack resistance of the material

With increasing microcrack density inside the process zone the bulk density of the material decreases. Thus after unloading of a specimen the increased bulk volume of the process zone is pressed together by the surrounding less damaged material.

This is evident from the isochromatic pattern surrounding the process zone of an unloaded 4-point-bend specimen of a nuclear graphite shown in Fig. 3. In this Figure a photoelastic coating was glued onto the specimen /9/. Fig. 4 shows an analysis of the isochromatic pattern in view of the difference of the principal strains. It can be seen from this Figure that a region of high principal strain exists in front of the artificial notch and in addition a displacement of the neutral axis of more than 3 mm during loading the specimen up to the point of K_{Io} the beginning of stable crack growth. The non-linear non-elastic deformation ahead of a growing crack is a measure of microcracking indicating the increase of crack resistance during slow crack growth which was measured separately with a CT-specimen of the same material /10/.

As known from the literature, slow crack growth in coarse-grained ceramics /1, 8-11/ and in concrete /2, 3/ is generally accompanied by an increase of the crack resistance. However, this increase can be accomplished by both an increase of the size of the process zone and/or of the elastic potential of the process zone during microcracking.

The size of the process zone $2\,\psi_c$ depends on microstructural features such as the grain size as well as test conditions such as the loading rate. The most important feature on the microstructural scale is the distribution of the microcrack nuclei which is related to the size distribution of the most active facets, ie. those with the largest residual strains. In the case of e. g. alumina and concrete these most active facets are related to the largest grain as shown in the foregoing chapter. On the other hand in the case of a dispersion-toughened ceramic these most active facets are related to the facetted tetragonal zirconia grains. The size of the process zone $2\,\psi_c$ is also related to local microcrack field parameters. As shown by Gross /3/ the limit of the process zone becomes sharper as the density of the microcracks increases. This also depends on the microcrack configuration, but is generally due to unloading effects. As a measure in the case of rapid failure it was found experimentally that $2\,\psi_c$ in the case of high-strength fined-grained alumina and silicon carbide is in the range of some 100 µm /10/. In the case of concrete this value is in the range of some 100 mm /5/.

During slow crack growth with increasing crack resistance it was suggested by Wacharatane et al. /12/ that for mortar the value of $2\,\psi$ is nearly constant at about 75 mm. The same behaviour of the value of $2\,\psi$ during slow crack growth nearly holds for concrete /2/. Thus it must be concluded that with increasing microcrack density β during slow crack growth elastic interaction effects occur which contribute to strengthening the process zone of this class of materials. This will be explained in the following.

As shown with foregoing works /6/ the crack resistance of a brittle material is given by

$$J_R = \frac{S_m^2 \pi}{E\,4}\psi = \frac{2\,\gamma_s}{(2.5 - 1.5\,v - 4\,v^2)\,4\,a}\quad I_m^2\,\pi\,\psi \qquad \text{eq. (5)}$$

Thus it depends on the surface energy of a single microcrack multiplied by the square of the normalized strength of the microcrack system I_m^2 and the size of the process zone. E_m is the microcrack reduced Young's modulus of the process zone. It follows for the normalized Young's modulus

$$\frac{E_m}{E} = \frac{1}{1 + \beta K_{Im}/S_m \sqrt{\pi a}} \qquad \text{eq. (6)}$$

or vice versa the stress intensity factor of the microcrack system

$$\frac{K_{Im}}{S_m \sqrt{\pi a}} = I^{-1} = \sqrt{\frac{E - E_m}{\beta E_m}} \qquad \text{eq. (7)}$$

Hence an increase of the elastic potential of the process zone is equivalent to a decrease of the stress intensity factor of the crack system of the process zone.

Due to lack of space in this paper only the influence of two crack configurations on the crack resistance of the material will be discussed. As known from the literature, stress-induced microcracks ahead of a growing macrocrack are mostly arranged in a displaced orthogonal manner. This crack configuration can be analytically modelled with the diamond-like arrangement. The stress intensity factors of this crack system are ascertained by Gross /13/ as shown with Fig. 5. The Young's modulus of this crack system is calculated with eq. (7) and shown in Fig. 6. As a comparison the stress intensity factor of the statistically distributed crack system calculated with eq. (7) from values for the Young's modulus given by Budiansky et al /14/ is shown in Fig. 7. Here unloading effects are not taken into account and the strength of this crack system vanished at a crack density of about 0.6. However as seen in Fig. 5, unloading effects at high crack densities strengthen the process zone especially at high densities of parallel oriented crack. Thus special discrete distributions of microcrack nuclei can toughen ceramics as experimentally observed in the case of zirconia dispersed ceramics /6, 15/. On the other hand, in many ceramics for high-performance structural parts the microcrack nuclei are continuously distributed because in general each facet acts as a microcrack nuclei. Thus in this case the microcracks are mostly arranged in a collinear manner which gives rise to the so called crack branching. This is also observed in plain concrete. The strength of these kinds of crack systems is relatively low. A value in the range of the tension strength is found experimentally. This microcrack configuration has, if any, only a weak strengthening effect on the process zone.

Literature:

/1/ K. Kriz, F. W. Kleinlein: "Einfluß der Prüfgeschwindigkeit auf die langsame Rißausbreitung in Aluminiumoxid unterschiedlicher Korngröße", Ber. Dt. Keram. Ges. 57, 1980, 22

/2/ Ch. Sok, J. Baron, D. Francois: "Mécanique de la rupture appliquée au beton hydraulique", Cement and concrete research 9, 1979, 641-648

/3/ U. Diederichs, U. Schneider, M. Terrien: "Formation and propagation of cracks and acoustic emission", Fracture mechanics of concrete (ed. F. H. Wittmann), 1983, 157

/4/ S. Ziegeldorf, H. S. Müller, H. K. Hilsdorf: "Effect of Aggregate Particle Size on Mechanical Properties of Concrete", ICF 5, Vol. 5, 1981, 2243

/5/ S. Mindes: "The application of fracture mechanics to cement and concrete", Fracture mechanics of concrete (ed. F. H. Wittmann), 1983, 1

/6/ F. E. Buresch: "Macrocrack Extension in Microcracked Dispersion-Toughened Ceramics", Zirconia 83, MPI Stuttgart, 21.-23.6.1983, to be published in "Advance of Ceramics"

/7/ R. W. Davidge, J. R. McLaren, I. Titchell: "Statistical Aspects of Grain Boundary Cracking in Ceramics and Rocks", Fracture Mechanics of Ceramics, Vol. 5, 1983, 594

/8/ F. E. Buresch: "Relations between damage and microstructure of ceramics", Proc. Int. Symp. Eng. Ceramics, Jerusalem 1984, to be published

/9/ F. E. Buresch, K. Frye, Th. Müller: "Relationship between Microcrack Zones and Toughness of Fine Grained Alumina and Coarse Grained Graphite", Fracture Mechanics of Ceramics, eds. R. C. Bradt, A. G. Evans, D. P. H. Hasselman, F. F. Lange, Vol. 5, 1983, 591

/10/ F. E. Buresch, H. Nickel: "Mechanische Untersuchungen an keramischen Werkstoffen für Komponenten von Hochtemperatur-Reaktoren", DVM, Festigkeit keramischer Werkstoffe, Abschlußkolloquium im Schwerpunktprogramm der DFG, 1984, 123

/11/ R. Knehans, R. Steinbrech: "Effect of grain size on the crack resistance curve of Al_2O_3 bend specimens", Science of Ceramics, Vol. 12, 1984, 613

/12/ M. Wecharatana, S. P. Shah: "Nonlinear fracture mechanics parameters", Fracture Mechanics of Concrete, (ed. F. H. Wittmann), 1983, 463

/13/ D. Gross. "Spannungsintensitätsfaktoren von Rißsystemen", Ing. Arch. 51, 1983, 301-310

/14/ B. Budiansky, R. J. O'Connell: "Elastic Moduli of a Cracked Solid", Int. J. Solids Structures 12, 1976, 81 - 97

/15/ M. Rühle, W. M. Kriven: "Stress-induced transformations in composite zirconia ceramics", to be published, Ber. Bunsengesellschaft

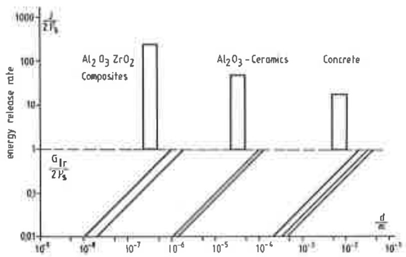

Fig. 1:
Normalized residual energy release rate $G_{Ir}/2\gamma_s$ vs grain/facet size distribution and characteristic values of normalized fracture energy release rate $J/2\gamma_s$; spontaneous microcracking for $G_{Ir} \geq 2\gamma_s$.

Table to Fig. 1: Material Parameter

		Al_2O_3-ZrO_2 composites	alumina ceramics	concrete	dimension
Young's modulus	E	250...350	350...400	25...37	GPa
residual strain	ε	$\gtrsim 10^{-2}$	$\sim 10^{-3}$	$\sim 5\times10^{-4}$	
spec. surface energy	γ_s	~ 1	~ 1	~ 6	N/m
size of process zone	$2\psi_c$	$\gtrsim 0.01$	$\gtrsim 0.1$	$\gtrsim 100$	mm
notch fract. strength	S_{mc}	$\gtrsim 1000$	$\gtrsim 100$	$\gtrsim 100$	MPa

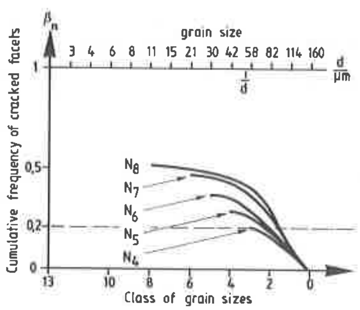

Fig. 2:
Cumulative cracked facets of a duplex microstructure vs grain size for different activated internal strain energy levels.

Fig. 3:
Isochromatic frings pattern in a birefringent coating around the damage zone in front of a artificial notch (arrow) after unloading from K_{Io} for a coarse grained graphite.

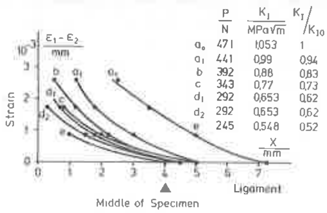

Fig. 4:
Differences of principles strains ahead of a rounded notch for a coarse grained graphite in 4-point bending.

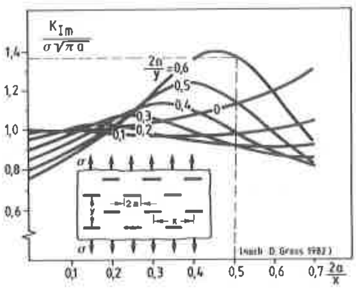

Fig. 5:
Stress intensity factor of the diamond-like crack system vs crack density (β_y, β_x) after Gross /13/.

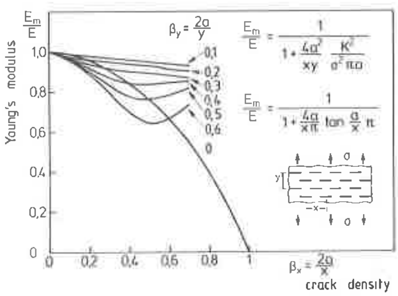

Fig. 6:
Young's modulus of a diamond-like crack system vs crack density (β_y, β_x)

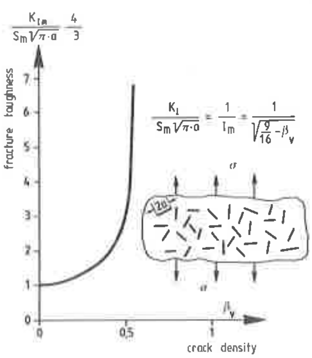

Fig. 7:
Stress intensity factor of the statistically oriented crack system vs crack density.